

SIZE EFFECT ASPECTS OF MEASUREMENT OF FRACTURE CHARACTERISTICS OF QUASIBRITTLE MATERIAL

Zdeněk P. Bažant

Walter P. Murphy Professor of Civil Engineering and Materials Science,
Northwestern University, Evanston, IL 60208, USA

Abstract

The paper, which represents the text of an introductory report presented at Cardiff workshop in 1995, reviews the size effect from two different viewpoints: 1) the need to eliminate or minimize the effect of specimen size on the measured material fracture characteristics, and 2) the exploitation of measured size effect on the nominal strength for determining the material fracture characteristics. Three methods of fracture testing are examined in the perspective of the size effect, and the merits and weaknesses of various methods in regard to the size effect are pointed out. The parameters of all three methods can be determined by simple formulas and linear regression from measurements allowing calibration of two parameters of the size effect law.

KEY WORDS: Concrete, quasibrittle materials, fracture mechanics, size effect, scaling, fracture testing, test specimens, standardization.

1 Introduction

The size effect on nominal strength of structures is the most important practical consequence of the global energy release associated with large fractures. Therefore it is natural to exploit the size effect for measuring material fracture properties. At the same time, the measured values of the parameters characterizing material properties must be independent of the

specimen or structure size, or else they would not represent properties of the material alone but also properties of the structure.

The objective of the present paper, which represents the text of an introductory report that was orally presented at the size effect session a recent workshop in Cardiff¹ on the subject and was summarized at subsequent workshop at FraMCoS-2², is to review the issues which were deemed³ to be most important or interesting for the problem of selecting a standardized fracture test. Presentation of a comprehensive state-of-art report, mathematical derivations and experimental validations are not the objective. No claims for exhaustiveness of the present review are made. Design and other aspects of size effect are not covered in this paper.

2 Two Aspects of Size Effect

The size effect impacts the problem of choice of a standardized fracture test in two ways:

1. *Size Independence of Fracture Characteristics: Objectivity Requirement.*—The material fracture parameters such as the fracture energy must be independent of the specimen size (and geometry), when geometrically similar specimens of different sizes are tested. It is the basic requirement of objectivity of a fracture model.
2. *Determination of Fracture Parameters from Size Effect Measurements.*—Measurement of the size effect on nominal strength of concrete specimens can be exploited for determining the fracture parameters. It is in fact desirable to do so because the size effect is the most important feature of fracture mechanics of quasibrittle materials, distinguishing it from other failure theories, and is the main reason why fracture mechanics needs to be introduced into design. If the designer is concerned mainly about size effect, he should calibrate the material parameters on the basis of measured size effect.

¹NSF Workshop on Standards for Measurement of Mode I Fracture Properties of Concrete, organized by B.I.G. Barr and S. Swartz, University of Wales, Cardiff, July 20–21, 1995.

²Workshop, co-ordinated by P. Rossi, on "Size Effects: Theoretical Concepts, Experimental Verification, and Implications for Design" at Second Int. Conf. on Fracture Mechanics for Concrete and Concrete Structures, held at 2nd International Conference on Fracture Mechanics of Concrete and Concrete Structures (FraMCoS-2), chaired by F.H. Wittmann), E.T.H., Zürich, July 26, 1995.

³Based on the reporter's correspondence before Cardiff workshop with the members of Working Group 3, having Z.P. Bazant and B. Karihaloo as co-chairmen and W. Gerstle, A. Maji, H. Mihashi, P. Perdikaris, V. Saouma, T. Tang and M. Tasdemir as members.

3 Test Methods Considered and Their Parameters

3.1 Work-of-fracture method [1]

This method, proposed for ceramics by Nakayama [2] and Tattersall and Taplin [3], was developed for concrete by Hillerborg [4]. It is based on the cohesive (or fictitious) crack model proposed for concrete by Hillerborg et al. [5]. This model is characterized by a stress-displacement curve $\sigma = \varphi(w)$ relating the cohesive (crack-bridging) stress σ to the crack opening displacement w . The two main parameters of the curve $\varphi(w)$ are: (1) the area under the complete curve, representing the fracture energy G_f^H (superscript H referring to Hillerborg), and (2) the initial slope of the curve which may be characterized by the area under the initial tangent representing the initial fracture energy G_f^I (Fig. 1) [41]. According to Planas, Elices and Guinea [6], one can also approximately identify as the third parameter the center of gravity of the area under the $\Phi(v)$ -curve, and the three parameters then suffice to uniquely characterize a bilinear softening curve $\Phi(v)$. The more detailed characteristics of the curve $\varphi(w)$ have little effect on the predicted fracture behavior of structures and can hardly be experimentally determined without ambiguity. So (aside from parameters E and f_t' which do not refer exclusively to fracture), the number of fracture parameters that can be meaningfully determined by this method is basically two, although perhaps a third parameter can be identified from tests in a crude approximate manner.

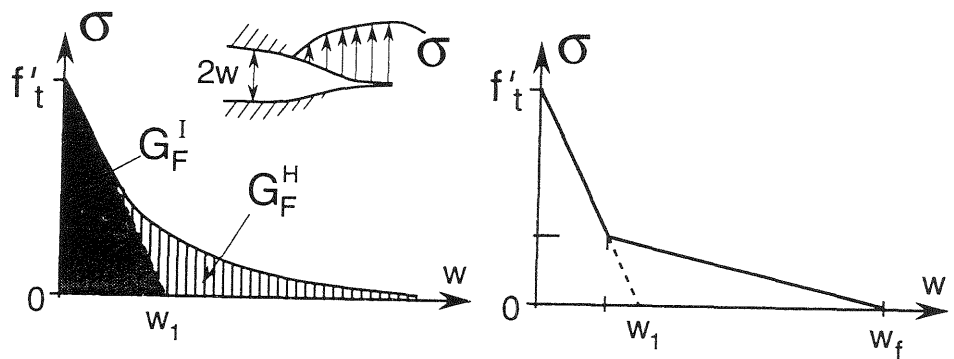


Figure 1: Softening stress-displacement law of cohesive (fictitious) crack model and its bilinear idealization

3.2 Size effect method

In this method [7], proposed for measuring fracture energy by Bažant [8] and Bažant and Pfeiffer [9] and for measuring two fracture parameters by Bažant and Kazemi [10], the basic fracture characteristics are: (1) the fracture energy, G_f^S (with superscript *s* referring to size effect method), and (2) the effective length of fracture process zone, c_f , defined as the distance from the notch tip to the tip of the equivalent LEFM crack in a specimen extrapolated (mathematically) to infinite size. The method is based on the size effect law proposed by Bažant [11,12], and particularly on its special form in terms of G_f^S and c_f and the dimensionless energy release rate function $g(\alpha)$, as proposed by Bažant and Kazemi [10] and Bažant and Cedolin [13].

3.3 Jenq-Shah method

This method is based on a fracture model proposed for concrete by Jenq and Shah [14], which is mathematically similar to the Wells-Cottrell model [15,16] for metals but has a very different underlying physical mechanism, with no plasticity. Same as the foregoing two models, this model contains two material fracture parameters: (1) the fracture toughness, K_{Ic}^{JS} (with superscript *JS* referring to Jenq and Shah), and (2) the critical crack-tip opening displacement δ_{CTOD}^S , which represents the opening displacement at the tip of notch (provided the fracture process zone remains attached to the notch). Instead of K_{Ic}^{JS} one can use the fracture energy $G_{Ic}^{JS} = (K_{Ic}^{JS})^2 / E'$ as one of the basic parameters.

Each of the fracture models underlying these methods is nonlinear and is completely or essentially defined by two parameters (G_f and f_t' , or G_f and c_f , or G_f and δ_{CTOD}^S). By contrast, LEFM has only one material parameter, either G_f or $K_{Ic} = \sqrt{E' G_f}$.

4 Extrapolation to Infinite Size: Unambiguous Definition of G_f etc.

Every test method is inevitably based on some material fracture model. A practical fracture model of a quasibrittle material represents a simplified description of a very complex process of progressive material damage and its localization in the fracture process zone. For this reason, the parameters

of any available fracture model to serve as a basis of standardized test can be truly unambiguously defined only by extrapolation to infinite size. Indeed, in a specimen of infinite size, the fracture process zone is negligibly small compared to the specimen size, which implies linear elastic fracture mechanics (LEFM) to be applicable; this in turn implies that the displacement field to which the fracture process zone is exposed along its boundary is the near-tip LEFM displacement field. This field is the same for any specimen geometry. Because the stress and strain fields in the interior of the fracture process zone must depend (in the sense of continuum smoothing) on the boundary displacements uniquely, they must also be the same. This guarantees the material fracture parameters defined on the basis of extrapolation to infinite size to be shape independent and, of course, size independent.

Thus, strictly speaking, an unambiguous definition of G_f^S , G_f^H , G_f^I , G_f^{JS} , c_f , K_{Ic} and δ_{CTOD} as true material properties, independent of specimen geometry and size, can be given only on the basis of extrapolation to infinite size.

5 Requirement of Size-Independence of Fracture Model Parameters

The fracture parameters obtained from the size effect law are, by definition, size independent. This is true not only for the specimens of the geometry used in tests but also for specimens of other geometries, because the same size effect law was shown to apply for specimens of very different geometries.

The parameters of Jenq and Shah model determined from the size effect law are of course size independent. If they are determined in the originally proposed way (with direct crack-tip opening displacement measurements), they appear to be approximately independent of the specimen size.

The fracture energy G_f^H , measured according to the work-of-fracture method on the basis of the area under the complete load-deflection curve of the specimen, was shown to be significantly size dependent. This appears to be a weakness of the cohesive crack model. The sources of this size dependence have been carefully analyzed by Guinea, Planas and Elices [19, 20], who also suggested how the size dependence of G_f^H could be mitigated.

As for G_f^I , it may be expected to be essentially size independent because it is approximately equal to G_f^S , which is size independent. Thus, the size dependence of G_f^H appears to be caused by the tail of the stress-displacement curve. The size dependence implies that the stress-displacement curve $\varphi(w)$ cannot be unique, contrary to the basic hypothesis of the cohesive crack model.

6 Ease of Determination of R-Curve for Given Structure Geometry

Other fracture characteristics, such as the R-curve, can be obtained from the aforementioned fracture characteristics. The R-curve, allowing the use of LEFM, represents the basis of the simplest method of structural analysis for fracture. Thus it is desirable that the fracture model would yield the R-curve in the most direct way possible.

This is achieved by the size effect method, for which the R-curve can be obtained from simple explicit expressions on the basis of G_f , c_f and the known energy release function for the given structure geometry. The formulas ensue from the size effect law because the R-curve is simply the envelope of fracture equilibrium curves for specimens of different sizes.

When Jenq-Shah model is used, the value of δ_{CTOD} may first be converted to c_f and then the R-curve can be calculated from the size effect by a known procedure. Another way, which is however equivalent, omits the explicit calculation of c_f and uses formulas giving the R-curve directly [17].

For the cohesive crack model, determination of the R-curve (curve of critical energy release rate R versus LEFM equivalent crack length a) is difficult; it requires nonlinear finite element analysis, which seems to be a disadvantage of this fracture model. (Nevertheless, a different type of R-curve, namely R versus CTOD, can be approximately calculated in a closed form [19, 20].)

7 Size Effect Method of Testing Material Fracture Parameters

7.1 Different versions of size effect method

The main advantage of the size effect method of measuring material fracture characteristics is the simplicity of measurement. Only the maximum loads of specimens need to be measured. For this purpose, sophisticated closed-loop systems and a stiff testing frame are not necessary. The measurements can be carried out in any laboratory, with the simplest equipment, and can be carried out even in the field, as demonstrated at the Texas Transportation Institute [22].

The second advantage of the size effect method is that the measurements are based on the same effect as that needed most for structural design. The model is calibrated by that effect which it is intended to predict.

In the original form proposed in 1987 [8,9], the size effect method has been amply verified and is now supported by broad experimental evidence.

Recently, in an effort to make testing more convenient, three new versions of size effect method have been formulated, and so four versions exist at present.

7.2 Original version with geometrically similar specimens of different sizes (Type I)

In the originally proposed version by Bažant [8] and Bažant and Pfeiffer [9], adopted as one of the RILEM recommendations [23], geometrically similar specimens of different sizes, spanning the size ratio at least 1:4, are tested. G_f^S and c_f are then determined either by nonlinear optimization or linear regression, along with their coefficients of variation.

For the original version, the size effect method has a third advantage: The identification of material parameters can be reduced to linear regression, and the regression can be arranged in such a way that the slope of the regression line gives the fracture energy. Linear regression is the most effective way to obtain good statistics, such as the coefficient of variation of the fracture energy, and the statistics are most dependable when the quantity of interest is the regression slope, as is the case for G_f^S .

For a material exhibiting such a high random scatter as concrete, determining the coefficients of variation of G_f and c_f is important. The design of structures should properly take this statistical information into account. It is one advantage of the size effect method that it makes determination of these coefficients of variation reliable and easy.

7.3 One-size version using zero-size strength (Type II)

In this recently proposed version, the maximum loads (or nominal strengths σ_N) of fracture specimens of only one size (and one geometry) are measured, and the nominal strength σ_p at zero-size (plastic) limit for specimens of this geometry is calculated according to plasticity from a known value of tensile strength f_t' . Then, using the size effect law, one finds that the fracture characteristics can be calculated from the formulas:

$$G_f = \frac{\sigma_p^2 D_0}{c_n^2 E} g(\alpha_0), \quad c_f = \frac{g(\alpha_0)}{g'(\alpha_0)} D_0 \quad (1)$$

in which

$$D_0 = \frac{D}{(\sigma_p / \sigma_N)^2 - 1} \quad (2)$$

and the nominal strength is defined as $\sigma_N = c_n P_{max} / bD$ where c_n is a factor chosen for convenience. The value of σ_p can be easily calculated according to Mohr-Coulomb yield criterion, assuming a bi-rectangular stress distribution along the ligament of the specimen, with stresses on one and the other side equal to the tensile and compressive strength. An ongoing research at Northwestern University by Zhengzhi Li (private communication [24]) has already shown that, for tensile strength equal to f_r , this method works very well for notched three-point-bend concrete fracture specimens of span-to-depth ratio 2.5, and gives results in good agreement with the original size effect method proposed by Bažant [8] and Bažant and Pfeiffer [9], provided that the notched specimens are large enough (a depth of 6 in. appears to suffice, but the larger the better).

There is, however, one aspect which must be handled empirically. The value of tensile yield strength f'_t , which is needed for calculating σ_p according to plasticity, is not predicted by fracture mechanics. By virtue of approaching for small sizes a horizontal asymptote, the size effect law implies σ_p to correspond to strength theory or plasticity but does not imply the proper value of f'_t to be the direct tensile strength, nor to be the same for various specimen geometries. In fact, upon equating the zero size limit $\sigma_p = B f'_t$ to $c_n [EG_f / c_f g'(\alpha_0)]^{1/2}$ where $B_p = B_p(\alpha_0) =$ nominal structure strength for unit value of material tensile yield strength calculated according to plasticity, one must conclude that the tensile yield strength value to be used must satisfy the relation:

$$f'_t = c_n \sqrt{EG_f / c_f g'(\alpha_0)} / B_p(\alpha_0) \quad (3)$$

This value is not constant. It varies with specimen geometry. Therefore, it is by chance that good results for the aforementioned specimens are obtained with $f'_t = f_r =$ modulus of rupture. For different geometries, different values of f'_t have to be used (e.g. $1.3f_r$ or $0.8f_r$). They would have to be calibrated

empirically for the geometry to be specified for the standard testing method. Although this is not difficult to do, it does mean that this method does not have a complete theoretical foundation but contains an empirical ingredient. This feature is not surprising because the size effect law $\sigma_N \propto [1+(D/D_0)]^{-1/2}$ is valid only within the approximate range $0.22 \leq D/D_0 \leq 4.5$, which excludes zero size.

7.4 One-size version using notchless specimen strength (Type III)

The aforementioned empirical ingredient can be avoided at the cost of slightly more complicated calculations. Instead of the zero-size limit, one can experimentally determine the strength of a notchless specimen, preferably (but not necessarily) of the same size and shape. This is similar to the standardized test of modulus of rupture, f_r . The size effect on f_r (Appendix II) must of course be taken into account simultaneously with the size effect for notched specimens. This can be accomplished by fitting the maximum load data with the universal size effect law in Eq. (12) of Appendix I, which is valid for both notched and notchless specimens. Under the assumption that $D_0 \gg D_b$ where D_b = thickness of the boundary layer in the modulus of rupture test (roughly one maximum aggregate size), which is normally satisfied, the universal law has recently been derived as the matched asymptotic satisfying the following asymptotic properties:

1. For notched specimens and $D_0 \gg D_0$, it agrees with the first three terms of the large size asymptotic series expansion and approaches the LEFM asymptote of slope $-1/2$ as $D \rightarrow \infty$.
2. For notched specimens and $D \ll D_0$, it agrees with the first two terms of the small-size asymptotic expansion and approaches a horizontal asymptote as $D \rightarrow 0$.
3. For notchless specimens, it reduces to the recently derived size effect for the modulus of rupture, agreeing well with test data of Bažant and Li [26].

Because this law differs from the original size effect law, the optimum fit of the classical data for notched specimens of different sizes of Bažant and Pfeiffer [9] is not exactly the same as published, but is very close.

The fitting of Eq. (12) to the measured nominal strength of notched and notchless specimens cannot be accomplished by linear regression. However, a computer library subroutine such as Levenberg-Marquardt nonlinear

optimization algorithm readily yields the values of G_f and c_f that provide the best fit.

Alternatively, iteration of linear regressions can also be used. Eq. (12) can be rearranged to the linear form $Y = A X + C$ in which

$$X = \frac{g}{g'} D, \quad Y = \frac{E c_n^2}{g' \sigma_N^2} \chi, \quad \chi = \left\{ 1 + \left[\left(\eta + \frac{4 g' D}{\langle -g'' \rangle c_f} \right) \left(1 + \frac{g D}{g' c_f} \right) \right]^{-1} \right\}^2 \quad (4)$$

and $A = 1 / G_f$, $C = c_f / G_f$ (note that for $\alpha_0 = 0$ we have $g = 0$ and $X = 0$). Parameter χ is assumed 1 for the first iteration and its value is then updated after each iteration of the linear regression. It has already established [26] that the iterations converge very well and that this method, which has a consistent theoretical foundation, gives excellent results, very close to those obtained by Bažant and Pfeiffer [9] with the original size effect method. Again, the higher the brittleness number of the notched specimens, the better the results. The specimen geometry and notch length should be chosen to as to minimize D_0 , that is, the ratio g' / g .

7.5 One-size version using notches of different length (Type IV)

As a generalization of the original size-effect method, the specimens need not be geometrically similar if the generalized size effect law in terms of $g(\alpha)$, G_f , and c_f [10] is used. However, the range of brittleness numbers $\beta = D / D_0$ must again be at least 1:4.

This formula offers the possibility to identify material fracture parameters from the maximum loads of specimens of only one size and the same external shape. This has recently been studied in depth by T. Tang et al. [22], with apparent success. However, it is not easy to achieve in this manner a sufficient range of β . Tang succeeded with eccentric compression specimens to achieve a range of about 1:4, which is the minimum required for meaningful approximate results. However, a notch as short as 1/8 of the cross-section depth had to be included to achieve this range of β . From recent research leading to Eq. (12) it appears that, for such a short notch, the simple size effect law has a significant error, which is according to Eq. (12) about 14% (approximately the same error magnitude for such a short notch would have to be expected for Jenq-Shah's model because it is approximately equivalent to the size effect law).

It would be of course possible to apply to such short notches the universal size effect law (12), which can describe the transition between specimens with large notches and no notches. But then one may as well use the measurement of the nominal strength of notchless beams, which is the method in Sec. 7.3, and in this way increase at the same time the range of β . But dissimilarity might cause some additional error because the LFM function $g(\alpha)$ accounts for the geometry effect only approximately.

7.6 Compromise with Reduced Number of Sizes

When two sizes of eccentric compression specimens that are similar but have two rather different relative notch depths α_0 are used and the size ratio is 1:2, one can reach a brittleness number range of about 1:6, and for three-point bend specimens about 1:4 (without using excessively short notches for which the transition to size effect on modulus of rupture would have to be considered). Both ranges are sufficient for measuring G_f and c_f .

8 Relationship Among Parameters of Different Models

Recently it has been shown that the Jenq-Shah method and the size effect method are mathematically equivalent within the first two terms of the asymptotic series expansion of the dimensionless energy release rate function $g(\alpha)$ in the size effect law. Because the higher-order terms of this expansion can get significantly manifested only for size ranges exceeding about 1:20, these two methods must be equivalent for practical purposes and their parameters must be related. Indeed, such a relation has been established by Bažant [27] and Bažant, Gettu and Kazemi [28] and may be written as follows:

$$K_{Ic}^S = \sqrt{g(\alpha_0)D_0} Bf'_i = \sqrt{E' G_f^S} \quad (5)$$

$$\delta_{CTOD}^S = \frac{\sqrt{8}}{\pi E'} \sqrt{g(\alpha_0)g'(\alpha_0)D_0} Bf'_i = \frac{\sqrt{8}}{\pi} \frac{K_{Ic}}{E'} \sqrt{c_f} = \frac{\sqrt{8}}{\pi} \sqrt{\frac{G_f^S c_f}{E'}} \quad (6)$$

where Bf'_i and D_0 are parameters of the size effect law $\sigma_N = Bf'_i [1 + (D/D_0)]^{-1/2}$, with $\sigma_N = P / bD$ ($c_N = 1$); $E' = E / (1 - \nu^2)$ for plane strain; α_0 = initial relative notch depth, and the values of c_f and G_f^S are the values obtained by

fitting maximum load data for notched specimens with the size effect law written in the form:

$$\sigma_N = \sqrt{\frac{E' G_f^S}{g'(\alpha_0) c_f + g(\alpha_0) D}} \quad (7)$$

where D = characteristic dimension (size) of specimen. The calculations are the simplest when the specimens are geometrically similar. However, the specimens need not be geometrically similar, since differences in geometry are captured by different values of $g(\alpha_0)$. Because of the typical scatter of test results for concrete, the range of brittleness numbers $\beta = D / D_0$ must be at least 1:4.

Extensive comparisons of test results by Karihaloo and Nallathambi [29,30] confirmed that

$$G_f^{NS} \approx G_f^S \quad (8)$$

As for the cohesive (fictitious) crack model of Hillerborg et al., it appears that, for normal concrete,

$$G_f^I \approx G_f^S \quad (9)$$

$$G_f^H \approx 2 G_f^S \quad (10)$$

which resulted from the simplified theoretical analysis of Planas and Elices [18]. In theory, one should expect G_f^H to be related not only to G_f^S but also to c_f , but this has not yet been researched. In a general cohesive crack model, the ratio G_f^H / G_f^I could of course have any value.

Accurate numerical calculations with the cohesive crack model show that the results closely follow the simple originally proposed size effect law [11,12] within size range 1:20. Thus, the values G_f^S and c_f which give about the same maximum loads as the cohesive crack model can be easily obtained by fitting this size effect law to the numerical results with the cohesive crack model. The inverse problem, namely determination of the cohesive crack model from the known size effect law is more difficult. Nevertheless, it transpires that, approximately, the value of G_f resulting from the size effect law determines the initial slope of the stress-displacement curve, and the value of c_f together with G_f^S ought to decide the area under the complete stress-displacement curve.

To predict the approximate softening stress-displacement curve of Hillerborg's fictitious crack model from size effect data, the curve may be assumed to be bilinear, with a knee at the height about $f'_t / 3$ (Fig. 1). The initial tangent aims at the point $w = w_1$ on the axis of displacement w , and the second straight line terminates on the w -axis at point w_f . Eqs. (9) and (10) are satisfied if

$$w_1 = 2 G_f^I / f'_t, \quad w_f = 2,5w_1 \quad (11)$$

In principle, however, c_f ought to be involved in these relations, but at present it is not known how.

It must be pointed out that for normal laboratory specimens the maximum load values calculated numerically (by finite elements) with the cohesive crack model are insensitive to the tail of the stress-displacement curve defining the cohesive crack model (this might not be quite true for specimens of high strength concrete and strong mortar). These maximum load values are sensitive only to the initial slope of the curve, which means they essentially depend only on G_f^I and not on G_f^H . On the other hand, the size effect on the ductility limit (snapback point on the calculated load-displacement diagram) does depend on G_f^H , but this relationship has not yet been explored systematically.

For a size range 1:1000, accurate finite element calculations of the maximum loads with the cohesive crack model show that a close fit by the size effect law requires its generalized form $\sigma_N = Bf'_t [1 + (D / D_0)^r]^{-1/2r}$ [1, 31, 32]. For short-notch three-point-bend beams, the optimum value is $r \approx 0.45$, but r depends strongly on geometry; e.g. for a large panel with a small central crack loaded by pressure on the crack, the optimum value of r appears to be about 1.5. Values of r differing from 1 do not seem important and necessary for the normal size ranges up to about 1:20.

9 Concluding Comment

Knowledge of the size effect on the failure load of fracture specimens, coupled with the effect of shape, is very useful for measuring fracture properties. On the other hand, the effect of size on the values of material fracture parameters must be avoided.

Appendix I. Universal Size Effect Law and Verification of One-Size Method

The universal size effect law [33,34] applicable to failures at both large cracks and crack initiation from the surface reads:

$$\sigma_N = B f_r^\infty \left(1 + \frac{D}{D_0}\right)^{-1/2} \left\{ 1 + \left[\left(\eta + \frac{D}{D_b} \right) \left(1 + \frac{D}{D_0} \right) \right]^{-1} \right\} \quad (12)$$

in which η = empirical constant of the order of 1 and, if we denote $g = g(\alpha_0)$, $g' = g'(\alpha_0)$, $g'_0 = g'(0)$, and $g'' = g''(\alpha_0)$,

$$f_r^\infty = c_N \sqrt{\frac{EG_f}{c_f g'_0}}, \quad D_0 = \frac{g'}{g} c_f, \quad D_b = \frac{\langle -g'' \rangle}{4g'} c_f, \quad B = \sqrt{\frac{g'_0}{g'}} \quad (13)$$

Eq. (12) can be proven by expressing σ_N^{-2} in terms of \mathcal{G} and expanding it into Taylor series in \mathcal{G} about point $\mathcal{G} = 0$. This yields the original size effect law if $\alpha_0 > 0$, and $\sigma_N / f_r^\infty = 1 + D_b / (D + \eta D_b)$ if $\alpha_0 = 0$. The latter differs from the recently published size-effect formula [35] for the modulus of rupture by constant η , but agreement with the first two terms of the asymptotic expansion in D^{-1} is not affected and good fit of test data is not compromised. Introducing constant η achieves that σ_N be finite for $D \rightarrow 0$, for both $\alpha_0 > 0$ and $\alpha_0 = 0$.

Eq. (12) represents the matched asymptotic satisfying 1) the first three terms of the large-size expansion in D^{-1} for notched specimens, 2) the first two terms of the small-size expansion in D for the notched specimens, and 3) the first two terms of the large size expansion in D^{-1} for notchless specimens.

Fig. 2 shows the surface of the universal size effect law for a typical three-point bend specimen (span-to-height ratio = 4). The empty points (circles) in the size effect regression plots in Figs. 3 and 4 show the data points from various published size effect tests based on the original size effect method (Type I) and the regression lines of these empty points. The solid (black) points are the mean experimental results for extrapolation to zero size (Type II method, Fig. 3) and for notchless specimens (Type III method, Fig. 4). The fact that the solid points are rather close to the regression lines of the empty points validates the one-size method. The one-

size method graphically means passing a regression line (not shown) through the solid point and the group of the empty points for one size D only. Obviously, if this is the st size for each of these test series, this regression line would be almost the same as the regression line of the empty points, and thus nearly the same G_f and c_f values will be obtained as with the original multi-size effect method.

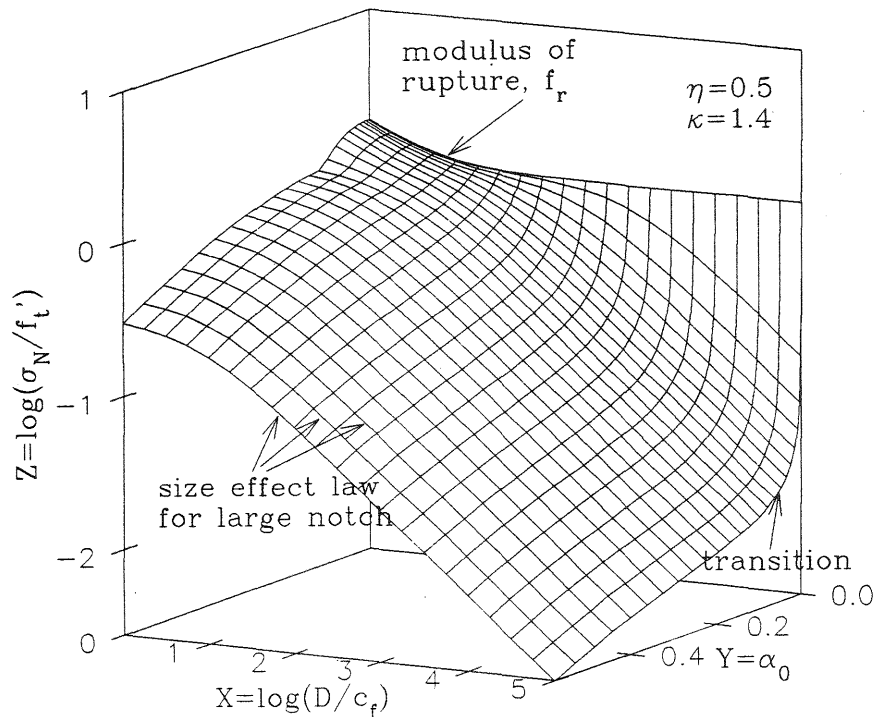


Figure 2: Surface of the universal size effect law for notched and notchless specimens

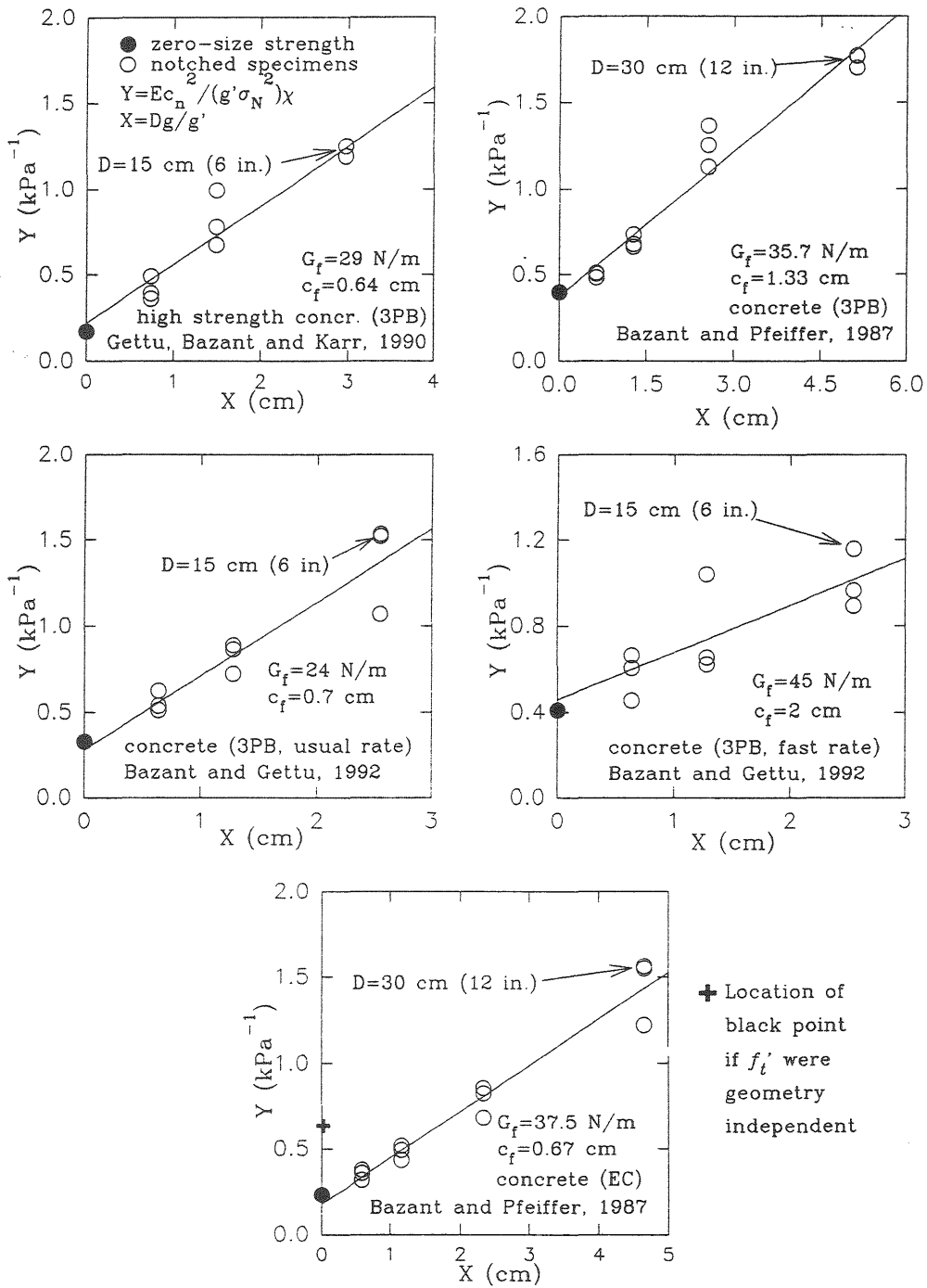


Figure 3: Size effect linear regression plots of typical published test data (empty points), their regression lines, and predictions by Type I method for zero size

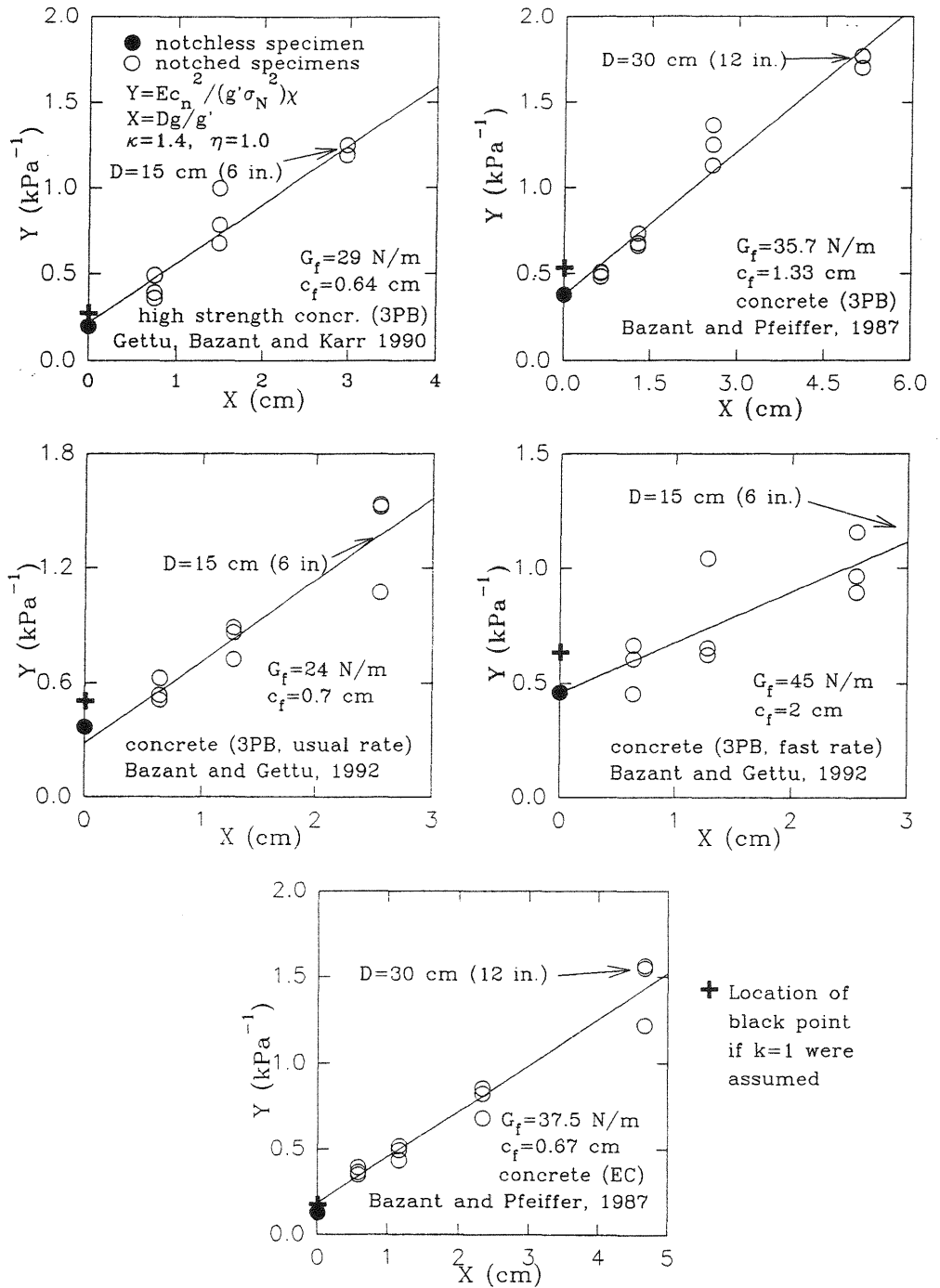


Figure 4: Size effect linear regression plots of typical published test data (empty points), their regression lines, and predictions by Type II method for notchless specimens

Appendix II. Other Kinds of Size Effect

1 Weibull Statistical Size Effect

Until about a decade ago, the size effect observed in concrete structures has been universally explained by randomness of strength and calculated according to Weibull theory. Recently, however, it has been shown [35] that this theory cannot apply when large stable fractures can grow in a stable manner prior to maximum load. The main reason is the redistribution of stresses caused by stable fracture growth prior to maximum load and localization of damage into a fracture process zone. If the Weibull probability integral is applied to the redistributed stress field, the dominant contribution comes from the fracture process zone whose size is nearly independent of structure size D . The contribution from the rest of the structure is nearly vanishing, which means the fracture cannot occur outside the process zone. Because this zone has about the same size for specimens of very different sizes, the Weibull-type size effect must, therefore, disappear for large sizes.

A generalized version of Weibull-type theory, in which the material failure probability depends not on the local stress but on the average strain of a characteristic volume of the material, has been shown to yield realistic size effect and also to approach the original size effect law as its deterministic limit [35].

For concrete, Weibull-type size effect might be taking place only in very large structures that fail right at crack initiation, for example, in very deep notchless plain concrete beams. Because for beam depths such as $D = 10 D_b$, the stress redistribution in the boundary layer, underlying Eq. (18), is still significant, the beam depth beyond which the Weibull-type size effect could begin to dominate must be at least $D = 100 D_b$. Hardly any case satisfying this condition exists in concrete practice. Besides, good practice requires designing structures so as not to fail at crack initiation. As for notched specimens, the Weibull size effect should, in theory, be approached for very small sizes, but the sizes for which this occurs appear to be too small, compared to the aggregate size.

2 The Question of Possible Role of Fractal Nature of Crack Surface or Microcrack Array

Although the surface roughness of cracks in concrete can be described, within a certain range, by means of a fractal curve, it appears according to Bažant that the fractality cannot play any significant role in the law of crack

propagation and especially not in the observed size effect on σ_N . Two reasons have been offered for this viewpoint [33,34]:

1. The size effect curve derived from the first and second law of thermodynamics disagrees with test data.
2. Distributed microcracking and plastic-frictional slips dissipate a major part of energy at the fracture while the microcracks that eventually become the final macro-crack surface exhibiting fractal features dissipate only a negligible portion of energy.

Since fractal curves such as von Koch's have been cited as paradigms of fractal cracks [36,37], it should further be noted that such curves generally exhibit recessive and spiraling segments which prevent kinematic separation of surfaces. However, this objection can be removed by considering self-affine fractal curves.

To circumvent the aforementioned criticism, it has been suggested [37] that the size effect may be caused by a different type of fractality, namely a lacunar (rarefying) fractal character of the distribution of microcracks in the fracture process zone (for which the fractal dimension is less than the Euclidean dimension). However, it can be shown that this type of fractal hypothesis can lead to nothing else than the Weibull-type size effect, with the fractality effect implied only in the values of Weibull parameters (which cannot be predicted theoretically anyway but must be calibrated by experiment). The reason is that if microcracks controlled failure, the failure would have to occur right at the start of macroscopic fracture growth, without any stable crack growth. Since the concrete structures of interest exhibit large stable crack growth, such a failure mode is an unrealistic hypothesis.

3 Diffusion size effects (drying, heating)

Diffusion phenomena such as water transport (drying) and heat transport caused by hydration and by environmental fluctuations engender time-dependent size effects, which must be avoided in fracture testing. To eliminate these size effects, all the specimens should have the same thickness. The drying size effect is also eliminated if the specimens are sealed during their curing and the test is made right after stripping the seals.

4 Wall effect

The wall effect is due to the fact that (1) the surface layer of concrete has a different aggregate content and size distribution than the interior, (2) the fluctuating microstresses normal to the surface are nonzero in the interior but zero on the surface, and (3) out-of-plane shear lips can develop at the surface ending of crack front edge. This has no appreciable influence on the observed size effect if the thickness of all specimens is the same.

Acknowledgment

Partial financial support from NSF under Grant MSS-911447-6 to Northwestern University and from the ACBM Center at Northwestern University is gratefully acknowledged.

References

1. ACI Committee 446 (1992). "State-of-art-report on fracture mechanics of concrete: concepts, models and determination of material properties." in *Fracture Mechanics of Concrete Structure*, ed. by Z. P. Bažant, Elsevier Applied Science, London, New York. 4–144.
2. Nakayama, J. (1965). "Direct measurement of fracture energies of brittle heterogeneous material." *J. of the Amer. Ceramic Soc.* **48** (11).
3. Tattersall, H.G., and Tappin, G. (1966). "The work of fracture and its measurement in metals, ceramics and other materials." *J. of Mater. Sci.* **1** (3), 296–301.
4. Hillerborg, A. (1985). "Theoretical basis of method to determine the fracture energy G_f of concrete." *Materials and Structures* **18** (106), 291–296.
5. Hillerborg, A. (1985). "Results of three comparative test series for determining the fracture energy G_f of concrete." *Materials and Structures* **18** (107).
6. Planas, J., Elices, M., and Guinea, G.V. (1993). "Cohesive cracks vs. nonlocal models: Closing the gap." *Report*, Techn. Univ. of Madrid; also *Int. J. of Fracture*, **63** (2), 173–187.

7. RILEM Recommendation (1990). "Size effect method for determining fracture energy and process zone of concrete." *Materials and Structures* **23**, 461–465.
8. Bažant, Z.P. (1987). "Fracture energy of heterogeneous material and similitude." Preprints, *SEM-RILEM int. conf. on Fracture of Concrete and Rock* (held in Houston, Texas, June 1987), ed. by S.P. Shah and S.E. Swartz, publ. by SEM (Soc. for Exper. Mech.), 390–402.
9. Bažant, Z.P., and Pfeiffer, P.A., (1987). "Determination of fracture energy from size effect and brittleness number." *ACI Materials Journal*, **84** (6), 463–480.
10. Bažant, Z.P., and Kazemi, M.T. (1990). "Determination of fracture energy, process zone length and brittleness number from size effect, with application to rock and concrete." *Int. J. of Fracture*, **44**, 111–131.
11. Bažant, Z.P. (1983). "Fracture in concrete and reinforced concrete," Preprints, IUTAM Prager Symposium on *Mechanics of Geomaterials: Rocks, Concretes, Soils*, ed. by Z.P. Bažant, Northwestern Univ., 281–316.
12. Bažant, Z.P. (1984). "Size effect in blunt fracture : concrete, rock, metal." *J. of Engineering Mechanics*, ASCE, **110**, 518–535.
13. Bažant, Z.P., and Cedolin, L. (1991). *Stability of structures: elastic, inelastic, fracture and damage theories* (textbook and reference volume), Oxford University Press, New York, 1991 (984 + xxvi pp.).
14. Jenq, Y.S., and Shah, S.P., (1985). "A two parameter fracture model for concrete." *Journal of Engineering Mechanics*, **111** (4), 1227–1241.
15. Wells, A.A. (1961). "Unstable crack propagation in metals-cleavage and fast fracture." *Symp. on Crack Propagation*, Cranfield, Vol.1, 210–230.
16. Cottrell, A.H. (1963). *Iron and Steel Institute Special Report* **69**, p. 281.
17. Ouyang, C., and Shah, S.P. (1991). "Geometry-Dependent R-Curve for Quasi-Brittle Materials." *J. of Amer. Ceramic Soc.* **74**, 2831–2836.

18. Planas, J., and Elices, M. (1989), in *Cracking and Damage*, ed. by J. Mazars and Z.P. Bažant, Elsevier, London, 462–476.
19. Planas, J., Guinea, G.V., and Elices, M. (1994). "Determination of the fracture parameters of Bažant and Jenq-Shah based on simple tests". Report to ACI-SEM Joint Task Group on Fracture Testing of Concrete, Universidad Politecnica de Madrid (June); **6**.
20. Guinea, Planas, J., and Elices, M. (1994). *Materials and Structures* **27**, 99–105 (also summaries in Proc., IUTAM Symp., Brisbane 1993 and Torino, 1994).
21. Planas, J., Elices, M., and Toribio (1989). in *Fracture of Concrete and Rock: Recent Developments*, ed. by S.P. Shah, S. Swartz and B.I.G. Barr, Elsevier Applied Science, London, 203–212.
22. Tang, T. (1994). Private communication to Z.P. Bažant, Texas Transportation Institute, Texas A&M University.
23. RILEM Recommendation (1985). "Determination of fracture energy of mortar and concrete by means of three-point bend tests of notched beams." RILEM TC 50-FMC, *Materials and Structures* **18** (106).
24. Li, Zhengzhi (1995). Private communication to Z.P. Bažant, Northwestern University.
25. Bažant, Z.P., and Li, Z. (1995). "Modulus of rupture: Size effect due to fracture initiation in boundary layer." *J. of Structural Engineering*, **121** (4), 739–746.
26. Bažant, Z.P., and Li, Z. (1996). "Zero-brittleness size effect method for one-size fracture test of concrete." *ASCE J. of Engrg. Mech.* **122**, in press; based on Report **94-12/603** (1994), Department of Civil Engrg., Northwestern University, Evanston, Illinois.
27. Bažant, Z.P. (1994). Discussion of "Fracture mechanics and size effect of concrete in tension. by T. Tang, S.P. Shah, and C. Ouyang, *J. of Structural Engineering ASCE*, **120** (8), 2555–2558. Bažant, Z.P. (1994)." Is size effect caused by fractal nature of crack surfaces?" Report **94-10/C402i**, Dept. of Civil Engrg., Northwestern University.

28. Bažant, Z.P., Gettu, R., and Kazemi, M.T. (1991). "Identification of nonlinear fracture properties from size effect tests and structural analysis based on geometry-dependent R-curve." *Int. J. Rock Mechanics and Mining Sciences*, **28** (1), 43–51.
29. Karihaloo, B. (1995). "Fracture mechanics and structural concrete." Longman, London.
30. Karihaloo, B.L., and Nallathambi, P. (1991). "Notched beam test: Mode I Fracture Toughness." in *Fracture Mechanics Test Methods for Concrete*, eds. S.P. Shah and A. Carpinteri, Chapman and Hall, London, 1–86.
31. Bažant, Z.P. (1985). "Comment on Hillerborg's size effect law and fictitious crack model." *Dei Poli Anniversary Volume*, Politecnico di Milano, Italy, ed. by L. Cedolin et al., 335–338.
32. Bažant, Z.P. (1985). "Fracture mechanics and strain-softening in concrete." Preprints, *U.S.- Japan Seminar on Finite Element Analysis of Reinforced Concrete Structures*, Tokyo, Vol. **1**, pp. 47–69.
33. Bažant, Z.P. (1995). "Scaling theories for quasibrittle fracture: Recent advances and new directions." in *Fracture Mechanics of Concrete Structures* (Proc., 2nd Int. Conf. on Fracture Mech. of Concrete and Concrete Structures (FraMCoS-2), held at ETH, Zürich), ed. by F.H. Wittmann, Aedificatio Publishers, Freiburg, Germany, 515–534.
34. Bažant, Z.P. (1995). "Scaling of quasibrittle fracture and the fractal question." *ASME J. of Materials and Technology* **117** (Oct.), 361–367 (Materials Division Special 75th Anniversary Issue).
35. Bažant, Xi, Y., and Reid, S.G. (1991). "Statistical size effect in quasi-brittle structures: I. Is Weibull theory applicable?, II. Nonlocal theory" *ASCE J. of Engineering Mechanics* **117** (11), 2609–2622.
36. A. Carpinteri, B. Chiaia and G. Ferro (1994) "Multifractal scaling law for the nominal strength variation of concrete structures," in *Size effect in concrete structures* (Proc., Japan Concrete Institute International Workshop, held in Sendai, Japan, 1993), ed. by M. Mihashi, H. Okamura and Z.P. Bažant, E & FN Spon, London-New York, 193–206.

37. A. Carpinteri and B. Chiaia (1995). "Multifractal scaling law for the fracture energy variation of concrete structures." *Fracture Mechanics of Concrete Structures* (Proceedings of FraMCoS-2, held at E.T.H., Zürich), ed. by F.H. Wittmann, Aedificatio Publishers, Freiburg (1995) 581–596.
38. Gettu, R., Bažant, Z.P., and Karr, M.E. (1990). "Fracture properties and brittleness of high strength concrete." *ACI Materials Journal*, **87**-M66, Nov., 608–618.
39. Kanninen, M.F., and Popelar, C.H. (1985). *Advanced Fracture Mechanics*, Oxford University Press, New York.
40. Jirásek, M., and Bažant (1995). "Macroscopic fracture characteristics of random particle systems." *Intern. J. of Fracture*, **69** (3), 201–228.
41. Bažant (1996). "Analysis of work-of-fracture method for measuring fracture energy of concrete." *ASCE J. of Engrg. Mechanics* **122** (2), 138–144.
42. Ožbolt, J., and Bažant (1996). "Numerical smeared fracture analysis: Nonlocal microcrack interaction approach." *Int. J. for Numerical Methods in Engrg.* **39**, 635–661.
43. Bažant, and Li, Yuan-Neng (1995). "Stability of cohesive crack model: Part II —Eigenvalue analysis of size effect on strength and ductility of structures." *Trans. ASME, J. of Applied Mechanics* **62** (Dec.), 965–969.
44. Bažant, Li, Z., and Thoma, M. (1995). "Identification of stress-slip law for bar or fiber pullout by size effect tests." *ASCE J. of Engrg. Mech.*, **121**(5), 620–625.
45. Bažant, and Jirásek, M. (1993). "R-curve modeling of rate and size effects in quasibrittle fracture." *Int. Journal of Fracture*, **62**, 355–373.
46. He, S., Plesha, M.E., Rowlands, R.E., and Bažant (1992). "Fracture energy tests of dam concrete with rate and size effects." *Dam Engineering* **3** (2), 139–159.